Authors' accepted manuscript: ISOCS/IEEE International Symposium on Olfaction and Electronic Nose (ISOEN) Fukuoka, Japan, 2019.

A Realistic Remote Gas Sensor Model for Three-Dimensional Olfaction Simulations

Dino Hüllmann[1*], Patrick P. Neumann[1], Javier Monroy[2] and Achim J. Lilienthal[3]
[1]*Bundesanstalt für Materialforschung und -prüfung (BAM)* Berlin, Germany
[2]*Machine Perception and Intelligent Robotics group (MAPIR), Universidad de Malaga*, Spain
[3]*Mobile Robotics & Olfaction Lab, AASS Research Center, Örebro University*, Sweden
*dino.huellmann@bam.de

***Abstract*—Remote gas sensors like those based on the Tunable Diode Laser Absorption Spectroscopy (TDLAS) enable mobile robots to scan huge areas for gas concentrations in reasonable time and are therefore well suited for tasks such as gas emission surveillance and environmental monitoring. A further advantage of remote sensors is that the gas distribution is not disturbed by the sensing platform itself if the measurements are carried out from a sufficient distance, which is particularly interesting when a rotary-wing platform is used. Since there is no possibility to obtain ground truth measurements of gas distributions, simulations are used to develop and evaluate suitable olfaction algorithms. For this purpose several models of in-situ gas sensors have been developed, but models of remote gas sensors are missing. In this paper we present two novel 3D ray-tracer-based TDLAS sensor models. While the first model simplifies the laser beam as a line, the second model takes the conical shape of the beam into account. Using a simulated gas plume, we compare the line model with the cone model in terms of accuracy and computational cost and show that the results generated by the cone model can differ significantly from those of the line model.**

***Index Terms*—gas simulation, remote gas sensor, TDLAS**

I. Introduction

Tasks such as accident assessment, environmental monitoring and surveillance of gas emissions from infrastructure such as pipelines, landfills and industrial plants often require the localisation of gas sources or the mapping of gas distributions in large outdoor environments, which are ideal applications for mobile robots with olfactory/gas sensors.

While in the past in-situ sensors were used most often on gas-sensing robots, remote gas sensors based on the Tunable Diode Laser Absorption Spectroscopy (TDLAS) are becoming increasingly popular. Unlike their in-situ counterparts, these sensors do not require direct contact with the gas and are therefore better suited for inspecting large outdoor areas.

However, in contrast to in-situ sensors which perform point measurements, TDLAS sensors measure the integrated gas concentration along the path of their laser beam (Fig. 1) and thus require the development of new algorithms for localising gas sources and mapping gas distributions. Since field experiments with gas dispersal are costly, lack ground truth data and repeatability, simulations are usually used to evaluate and compare such algorithms [1].

Several tools to simulate gas dispersion have been developed. In [2] a recent overview is given and a new simulator named GADEN is presented that provides sensor models of various in-situ gas sensors. Although TDLAS sensors have been characterised and used with robots to map gas distributions and to localise gas sources using 2D line and cone models ([3]–[5]), no realistic 3D sensor model exists yet.

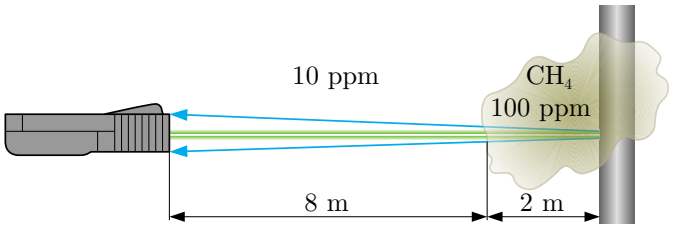

Fig. 1. TDLAS sensors measure an integrated gas concentration. Given a background concentration of 10 ppm, the shown measurement would read $8\,\mathrm{m} \cdot 10\,\mathrm{ppm} + 2\,\mathrm{m} \cdot 100\,\mathrm{ppm} = 280\,\mathrm{ppm} \cdot \mathrm{m}$.

In this paper we present two 3D TDLAS sensor models, a line and a cone model. While for the line model presented in Sec. II-A we make the simplification that the laser beam is a line, the cone model presented in Sec. II-B takes the conical shape and intensity profile of the beam into account. After generating a gas plume using GADEN, we compare the line model with the cone model (Sec. III) and discuss the results in Sec. IV.

II. TDLAS Sensor Models

Usually, simulation tools store both the gas distribution and obstacles in the environment discretely in grid cells. The pose of the sensor within the grids is described by its position, $\vec{p}$, and its direction vector, $\vec{n}$. To fully describe the characteristics of a TDLAS sensor, two additional parameters are required: the maximum measurement distance, L_{max}, and the divergence of the beam, θ. From the latter the total angular spread as shown in Fig. 3 can be computed as $\Theta = 2\theta$.

Often, the manufacturers of TDLAS sensors specify a spot diameter at a specific distance in their data sheets instead of the beam divergence, but these values can be easily converted into each other.

A. Line Model

For the first TDLAS sensor model we neglect the conical character of the laser beam and assume a line shape. Two steps have to be performed to obtain a measurement.

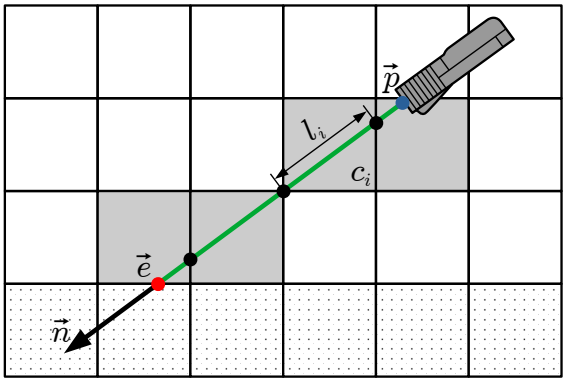

Fig. 2. Raytracing of a TDLAS beam through a 2D grid. The dotted cells represent obstacles, the grey cells are considered for the concentration estimation, the blue/red dot marks the start/end point of the ray and the black dots mark the intersection points of the ray with the gas concentration grid.

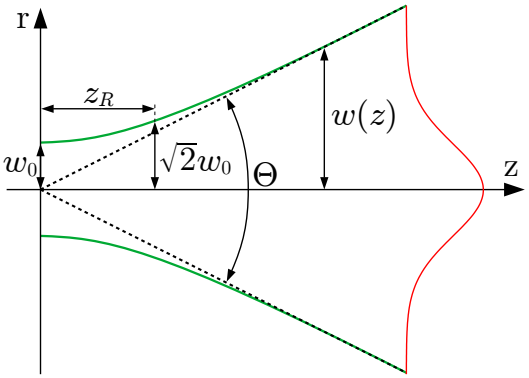

Fig. 3. Parameters of a Gaussian beam with propagation in z-direction. The red curve shows the Gaussian intensity profile of the beam. At a radial distance $w(z)$ from the centre of the beam, shown by the green curves, the intensity drops to $1/e^2$ of the centre value. Θ is the total angular spread of the beam.

First, the cells representing the environment are traced until either an obstacle is hit or the maximum measurement distance of the sensor is reached. If an obstacle is hit, the intersection point defines the end point of the measurement ray, which is given as $\vec{e} = \vec{p} + L \cdot \vec{n}$ with L denoting the length of the ray as shown in Fig. 2. Otherwise the measurement becomes invalid since a reflective surface is missing.

If the environment ray trace was successful, a ray through the gas concentration cells is traced from $\vec{p}$ to $\vec{e}$. With l_i denoting the path length traversed in cell i and c_i denoting the concentration in cell i, the measured concentration becomes

$$C = \sum_{\vec{p}}^{\vec{e}} c_i \cdot l_i + \varepsilon \tag{1}$$

with $\mathrm{ppm} \cdot \mathrm{m}$ as its unit and ε denoting the sensor noise, which we will neglect for the considerations in this paper.

B. Cone Model

The simplification we made for the line model does not hold in the real world since laser beams have a conical shape with a Gaussian intensity distribution, which is taken into account by the cone model. The basic idea is to approximate the conical shape by performing multiple single line measurements.

The intensity of a Gaussian beam is given by [6]

$$I(r,z) = I_0 \left(\frac{w_0}{w(z)}\right)^2 \exp\left(\frac{-2r^2}{w(z)^2}\right), \tag{2}$$

where z is the axial distance in the direction of propagation from the waist of the beam at $z = 0$, r is the radial distance from the centre of the beam, $w(z)$ is the beam radius at which the intensity drops to $1/e^2$ of the value at the centre and w_0 is the waist radius, i.e. $w_0 = w(0)$, as shown in Fig. 3. $w(z)$ is also known as the spot size parameter and is computed as

$$w(z) = w_0 \sqrt{1 + \left(\frac{z}{z_R}\right)^2}, \tag{3}$$

where z_R is the Rayleigh range [6].

The Rayleigh range is given by

$$z_R = \frac{\pi w_0^2}{\lambda}, \tag{4}$$

with λ denoting the wavelength.

As mentioned above, most manufacturers of TDLAS sensor devices specify the spot diameter at a specific distance z_{ds} in their data sheets. From this diameter we compute the spot radius $r_{ds} = w(z_{ds})$. By inserting (4) into (3) a solution for w_0^2 can be computed:

$$w_0^2 = \frac{w(z)^2}{2} - \sqrt{\left(\frac{w(z)^2}{2}\right)^2 - \left(\frac{z\lambda}{\pi}\right)^2}. \tag{5}$$

A typical TDLAS sensor for methane has a wavelength of $\lambda = 1653\,\mathrm{nm}$ and a spot diameter of 56 cm at 30 m distance yielding a waist radius of $w_0 \approx 56\,\mu\mathrm{m}$.

The orientation of each measurement ray, $\vec{r}_j$, is defined by its polar angle ϑ_j and its azimuthal angle φ_j with respect to the direction vector of the sensor, $\vec{n}$. Thus the radial distance of ray j from the centre axis of the beam at a distance z is given as $r_j(z) = z \cdot \sin(\vartheta_j)$.

By inserting this into (2) the integrated intensity of each ray can be computed as

$$I_j = I_0 \frac{1}{L_j} \int_0^{L_j} \left(\frac{w_0}{w(z)}\right)^2 \exp\left(\frac{-2z^2 \sin^2(\vartheta_j)}{w(z)^2}\right) dz, \tag{6}$$

where L_j denotes the length of ray j.

Since no analytical solution exists for this integral, we compute an approximation while tracing through the grid using the beam width in the middle of the path through the corresponding cell.

We use the integrated intensity of each ray to weight its contribution. With C_j denoting the concentration measured by ray j, the overall measurement result becomes

$$C = \frac{1}{\sum_j I_j} \sum_j I_j \cdot C_j. \tag{7}$$

III. TDLAS Sensor Model Comparison

To compare the simplified line with the cone model a gas release of methane with a cell size of 0.1 m is simulated with GADEN yielding the plume shown in Fig. 4. The point source of the plume is located at $(0, 0, 0)$ m and the plume propagates along the x axis, which is the main wind direction. Starting from $(0\,\mathrm{m}, 0\,\mathrm{m}, z)$ the sensor is moved to $(6.5\,\mathrm{m}, 0\,\mathrm{m}, z)$ with a step size of 0.1 m. This process is repeated at three different heights above ground, $z = [5, 15, 25]$ m. Moreover, we tested several sensor configurations which are shown in Tab. I. For example, configuration a) corresponds to the line model and configuration b) is the cone model with four rays ($\vartheta_0 = 0, \varphi_0 = 0$, $\vartheta_{1,2,3} = \theta/2$, $\varphi_{1,2,3} = [0, 120, 240]°$). In Fig. 4 the concentration measurements for some sensor configurations at heights of 5 m and 25 m are shown.

Sensor configuration e) with a total number of 131 rays is used as reference to compare the results. Tab. I shows the root mean square error (RMSE) and the maximum error of the experiments with respect to sensor model e). In addition, the computing time of each experiment is shown. Here the longest experiment, which is model e) at a height of 25 m, defines the value of 100 %.

IV. Discussion and Conclusion

As expected, the sensor models become more accurate the more complex they are. For instance, while the line model has a relative error of up to 18%, cone model c) with 9 rays merely exceeds a relative error of 4%. On the other hand, the required computing time raises with increased complexity of the model. For example, sensor model e) takes more than 14 times longer to compute than model c) and thus correlates with the number of rays ($131/9 \approx 14.6$) in terms of computing time.

However, it is not just the number of rays playing a role, but also their geometry, as a comparison of model c) and d) shows. Therefore, future work will include finding a good geometry to generate accurate results with as few rays as possible. Depending on the application, using the line model might be sufficient, but especially at higher distances the cone model can yield significantly better results.

TABLE I
Root mean square error, relative error and computing time for different sensor configurations.

	Ray configuration	Height [m]	RMSE [ppm·m]	Rel. error [%]	Time [%]
a)	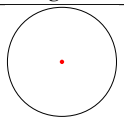	5 15 25	1.10 1.16 1.48	12.9 13.6 18.1	0.2 0.5 0.9
b)	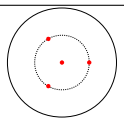	5 15 25	0.60 0.66 0.90	7.0 7.7 11.0	0.8 1.9 3.1
c)	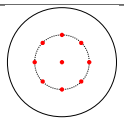	5 15 25	0.23 0.28 0.34	2.7 3.3 4.1	1.6 4.3 7.0
d)	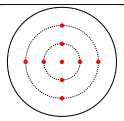	5 15 25	0.35 0.38 0.49	4.0 4.5 5.9	1.7 4.3 7.0
e)	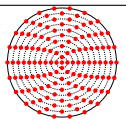	5 15 25	0	0	23.2 61.5 100.0

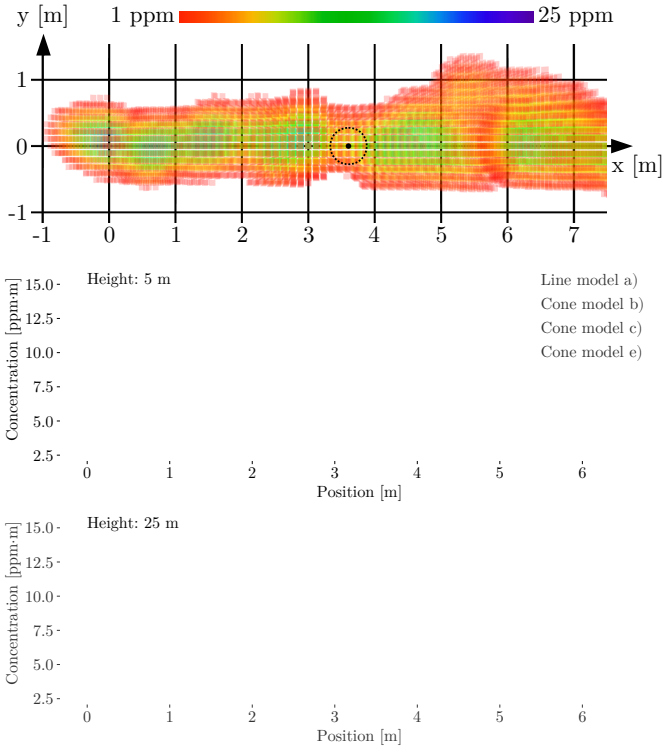

Fig. 4. Top: A simulated gas plume flowing from (0,0) in x-direction. The dashed circle illustrates the size of the beam of a typical TDLAS sensor at 30 m distance, the smaller spot inside at 5 m distance. Bottom: Plots showing the measured concentration along the plume with different sensor configurations at 5 m and 25 m above ground.

References

[1] H. Fan, M. A. Arain, V. Hernandez-Bennetts, E. Schaffernicht and A. Lilienthal, "Improving Gas Dispersal Simulation for Mobile Robot Olfaction: Using Robot-Created Occupancy Maps and Remote Gas Sensors in the Simulation Loop," International Symposium on Olfaction and Electronic Nose (ISOEN), 2017.

[2] J. Monroy, V. Hernandez-Bennetts, H. Fan, A. Lilienthal and J. Gonzalez-Jimenez, "GADEN: A 3D Gas Dispersion Simulator for Mobile Robot Olfaction," Sensors, vol. 17, no. 7, p. 1479, 2017.

[3] V. Hernandez-Bennetts, E. Schaffernicht, T. Stoyanov, A. Lilienthal and M. Trincavelli, "Robot Assisted Gas Tomography - Localizing Methane Leaks in Outdoor Environments," IEEE International Conference on Robotics and Automation (ICRA), 2014.

[4] P. P. Neumann, H. Kohlhoff, D. Hüllmann, A. Lilienthal and M. Kluge, "Bringing Mobile Robot Olfaction to the Next Dimension – UAV-based Remote Sensing of Gas Clouds and Source Localization," IEEE International Conference on Robotics and Automation (ICRA), 2017.

[5] S. Dierks and A. Kroll, "Experimental Characterization of a Tuneable Diode Laser Absorption Spectroscopy Based Sensor," IEEE Sensors Applications Symposium (SAS), 2018.

[6] O. Svelto, "Principles of Lasers", 5th edition, Springer, 2010.